Evolving land-atmosphere interactions over North America from CMIP5 simulations

Paul A. Dirmeyer*

George Mason University, Fairfax, Virginia, USA

Center for Ocean-Land-Atmosphere Studies, Calverton, Maryland, USA

Yan Jin, Bohar Singh, and Xiaoqin Yan

George Mason University, Fairfax, Virginia, USA

*Corresponding author address:

Center for Ocean-Land-Atmosphere Studies
4041 Powder Mill Road, Suite 302
Calverton, MD 20705-3106 USA
dirmeyer@cola.iges.org

For Submission to:

J. Climate CMIP5 special collection on North American climate

11 July 2012

1 **Abstract:**

2 Long-term changes in land-atmosphere interactions during spring and summer are

3 examined over North America. A suite of models from the Coupled Model

4 Intercomparison Project Phase 5 (CMIP5) simulating pre-industrial, historical and

5 severe future climate change scenarios are examined for changes in soil moisture,

6 surface fluxes, atmospheric boundary layer characteristics and metrics of land-

7 atmosphere coupling.

8 CMIP5 simulations of changes from pre-industrial to modern conditions show

9 warming brings stronger surface fluxes at high latitudes, while subtropical regions

10 of North America respond with drier conditions. There is a strong response in mid-

11 latitudes associated with anthropogenic aerosols, which reduce surface radiation

12 and heat fluxes, leading to a shallower boundary layer and lower cloud base. Over

13 the Great Plains the signal does not reflect a purely radiatively-forced response,

14 showing evidence that the expansion of agriculture may have altered land surface

15 properties in a way that offsets the aerosol impacts on the surface energy and water

16 cycle.

17 Future changes show soils are projected to dry across North America, even though

18 precipitation increases north of a line that retreats poleward from spring to summer.

19 Latent heat flux also has a north-south dipole of change, increasing north and

20 decreasing south of a line that also moves northward with the changing season.

21 Metrics of land-atmosphere feedback increase over most of the continent, but are

22 strongest where latent heat flux increases in the same location and season where

23 precipitation decreases. Combined with broadly elevated cloud bases and deeper

1   boundary layers, land-atmosphere interactions are projected to become more

2   important in the future, with possible consequences for seasonal climate prediction.

3

1. Introduction

A large number of studies with regional and global models and observed data sets over the last three decades have demonstrated that the state of the land surface has a significant influence on the atmosphere. Soil moisture is the most important land surface state variable affecting the global atmosphere on intraseasonal to interannual time scales (Dirmeyer 2011a). Climate modeling and observational studies have shown that a large portion of North America demonstrates a feedback of the land surface onto the atmosphere during summer (e.g., Koster et al. 2004; Findell et al. 2011). Guo et al. (2011) showed that potential predictability from soil moisture is high over North America. North America also demonstrates the strongest improvement in prediction skill from the realistic initialization of the land surface for seasonal forecasts (Koster et al. 2011). The location of maximum land-atmosphere coupling can vary in space (Koster et al. 2011) and its strength can vary from year to year (Guo and Dirmeyer 2012) depending on the pattern of the climatology of soil moisture and the fluctuation of its anomalies.

These results raise questions. Have the interactions between land and atmosphere changed since pre-industrial times, when atmospheric composition, aerosol loading, and global vegetation cover were different? More importantly, will land-atmosphere interactions change in the future? The Coupled Model Intercomparison Project Phase 5 (CMIP5; Taylor et al. 2012) provides an opportunity to address these questions in a multi-model framework.

This study has been conducted under the aegis of the "CMIP5 Task Force" coordinated under the Modeling, Analysis, Prediction and Projection (MAPP) program of the National Oceanic and Atmospheric Administration (NOAA) Climate

1   Program Office. The overall goal of the task force is to evaluate CMIP5 simulations of

2   the 20th century climate specifically over North America, as well as the character of

3   long-term predictions and projections of future climate. This study focuses

4   specifically on the developing role the land surface and land-atmosphere

5   interactions in a changing climate over North America. We focus on the spring and

6   summer seasons, because previous research indicates these are the most crucial for

7   land-climate interactions in this region and their impact on predictability and

8   prediction on sub-seasonal to seasonal time scales (e.g., Dirmeyer et al. 2009; Guo et

9   al. 2012).

10   Section 2 describes the data used and the techniques for estimating metrics and

11   indices of land-atmosphere interaction from the model simulations. Results and

12   synthesis are given in sections 3 and 4. A discussion and conclusions are presented

13   in section 5.

14

15   **2. Data and Techniques**

16   Monthly mean output fields from land and atmospheric data sets from 15 models

17   are used. Table 1 lists the models examined in this study. The choice of models was

18   predicated on several factors. Most important was the availability of a complete set

19   of necessary model output variables from a single ensemble member for each of

20   three simulations: the pre-industrial experiment (past), the historical experiment

21   (present), and the 8.5 Wm^{-2} representative concentration pathways (RCP85)

22   experiment (future). For each, we use 95 years of model output for calculation of

23   statistics and land-atmosphere coupling metrics. For the historical run, that

corresponds to the period 1911-2005 in the simulation. For the pre-industrial and RCP85 simulations, we chose the last 95 years of the available time series of data. The data within each 95-year time series is detrended so that statistics such as interannual standard deviations and temporal correlations between variables emphasize the short-term (interannual) variability characteristic of land-climate interactions. This also ensures the comparisons between experiments are consistent, since the historical run likely has an inherently significant trend that the other two experiments should not. The RCP85 projection is chosen over other less severe climate change scenarios with the rationale that signals not evident in this run must also be absent from the other projections, so this case should provide a sort of "upper bound" on coupled land-atmosphere responses in the CMIP5 dataset. The variables used in this study are the soil wetness in the top 10cm of the soil column, surface sensible and latent heat fluxes, near surface temperature and relative humidity (nominally 2m above ground level). We do not analyze precipitation, as we are concerned here with what may be considered the upward branch of the hydrologic feedback loop between land and atmosphere. Precipitation is the principal hydrologic input to the land surface, at the opposite end of the "cycle" from the land surface feedback to the atmosphere. Because of the complex and non-linear nature of convective processes, it is very difficult to discern the effect of the land surface on precipitation without carefully constructed sensitivity studies (cfr. Koster et al. 2006; Guo et al. 2006) that are beyond the scope of CMIP5.

All statistics are calculated separately for each month over a 95-year period and then averaged to seasonal values. All calculations are performed on each model's native grid, for only ice-free land points based on each model's land-sea-ice mask.

1   The data from each model are then interpolated bi-linearly onto the operational grid

2   of the European Centre for Medium-range Weather Forecasts (ECMWF) operational

3   forecast model, which is T1279 or a regular longitude-latitude grid of 2560x1280

4   grid boxes. This is a much higher resolution than any of the CMIP5 models, thus

5   ensuring no information content is lost in the process of interpolating down to

6   lower resolution grids, or via inadvertent smoothing when interpolating to a shifted

7   grid of similar resolution. We retain only the grid points on the high-resolution grid

8   that overlay land grid boxes of more than 80% of the CMIP5 models.

9   In addition to basic means and inter-annual standard deviations of the model output

10   variables, we calculate several derived terms to investigate land-atmosphere

11   interactions in the CMIP5 simulations. These include one-month lagged

12   autocorrelations for soil moisture (soil moisture memory), un-lagged correlation

13   between variables, and the terrestrial coupling index of Dirmeyer (2011b):

$$I(w_m, \phi_m) = \frac{\sum (w'_{m,y} \phi'_{m,y})}{\sqrt{\sum (w'_{m,y})^2}}$$

14   (1)

15   where w is the soil moisture and ϕ is either the sensible heat flux or the latent heat

16   flux. Primes denote anomalies from the mean annual cycle, and the correlations are

17   calculated for each month m across the 95 years y of available data. This index is

18   mathematically equivalent to the product of the standard deviation of the flux and

19   the correlation between soil moisture and the flux (Guo et al. 2006), and has the

20   same units as the flux (Wm^{-2}). Variables relevant to the atmospheric boundary layer

21   are also derived, including the height of the lifting condensation level:

22     $$Z_{LCL} = (T_{2m} - T_{D2m})/(\Gamma_{Dry} - \Gamma_{Dew}) \cong 125(T_{2m} - T_{D2m}) \qquad (2)$$

1   where 2m dew point T_{D2m} is estimated from near-surface relative humidity,

2   temperature T_{2m} and the mean surface pressure. Standard lapse rates Γ are used.

3   Relative humidity is converted to specific humidity q_{2m} for several of our analyses as

4   well. Finally, we estimate the local mean value of the Priestley-Taylor coefficient

5   based on the formulation of Betts (2004):

6
$$\alpha = \left(\frac{\lambda E}{H + \lambda E}\right)\left(\frac{1+\varepsilon}{\varepsilon}\right), \quad \varepsilon = \frac{\lambda}{C_P}\frac{dq}{dT}\bigg|_{T_{LCL}} \tag{3}$$

7   When combined with information from the other calculations, variations in α can

8   suggest how entrainment at the top of the growing daytime boundary layer may be

9   changing relative to bulk aerodynamic and canopy resistances at the surface

10 (Lhomme 1997).

11 It should be noted that we are using monthly mean model output to estimate

12 quantities initially derived and applied on instantaneous (Z_{LCL}), daily (I_{LH}) and 5-day

13 mean (α) data. Virtually all important land-atmosphere interactions are strongly

14 tied to the diurnal cycle, but time-averaged data can be used conscientiously to

15 tease out these processes (e.g., Betts 1994, 2004). Given the large spatial scales and

16 long time series of this study, gross features and changes should be discernable

17 from monthly data (Dirmeyer 2006).

18 One problem that cannot be ignored is the issue of spurious change signals in multi-

19 model means from CMIP model data. Figure 1 gives an example from our current

20 analysis. The difference in soil moisture between historical and pre-industrial

21 experiments for JJA is shown. The results from the 15 individual models are shown

anonymously in (a) and their unweighted average is given in (b). Certain features of
the multi-model mean are not robust across models, such as the wetter conditions
over the far western continental U.S., or the drying in the central Great Plains. The
inter-model standard deviation (c) indicates these two areas have the least
agreement among models. For instance, it appears the wet signal over California and
Nevada is almost entirely due to the bottom model in the center column.

As a result, we choose to use the degree of consensus among models for the sign of
the change (d) as the primary indicator of climate change responses. The coloring
shows the number of models out of 15 that agree on a change of a given sign. We see
that the drying signals over Mexico, the St. Lawrence valley, the northern Great
Plains and Northwest Territories of Canada are indeed robust, but the drying over
the north-central U.S. does not have widespread consensus.

The consensus approach also lends itself to straightforward estimation of statistical
significance. We can treat each model's projected change at each location as having
equal probability of an increase or decrease. Under this null hypothesis, the
expected probability of any particular number of models agreeing, or more than a
certain number agreeing, follows directly (see Table 2). For instance, the likelihood
of 11 or more models randomly agreeing on a positive or a negative change is
11.84% (2×5.92%).

Local probabilities have limited meaning without a concept of the field significance.
Dirmeyer et al. (2012a) determined that for the land surface variables considered
here, there are about 200 spatial degrees of freedom across all ice-free land points.

The entirety of North America displayed in all plots in this study constitutes approximately 17% of the global ice-free land area as depicted in the high-resolution grid used for these analyses. Assuming the spatial scale of variability is relatively uniform between continental and global scales, we estimate 34 spatial degrees of freedom for North America. With this estimate, we can calculate the field significance based on a set of 34 "events" where the outcome of each is based on the "cumulative probability" row of Table 2, thereby determining how much we must exceed the expected areal coverage of a given change at a given level of consensus to have confidence of a certain degree. The last row shows the thresholds that need to be met for areal coverage to be significant at the 99% confidence level. Based on these statistics, 71% or more of North America would have to be covered by at least a minimum (8:7) model consensus change of the same sign to be considered significant. We only check for significance of exceedance on the tails of the probability distribution – one could also test the likelihood of being significantly below the expected fraction of area as well.

3. Results

Calculations and significance testing has been performed on all fields and metrics for both past (historical minus pre-industrial) and future (RCP85 minus historical) cases. However, the results presented here will focus more on the future changes than the past, which are stronger and more significant in most cases. Where past

1 changes suggest significant or interesting results, and where they have some

2 bearing on our interpretation of future projections, they are also shown.

3 Figure 2 shows the multi-model mean soil moisture from the historical run for MAM

4 and JJA (top row), and the past (middle) and future (bottom) changes, represented

5 as the sign of the change and the degree of consensus among models. The right

6 middle panel is the same as Fig 1(d). The mean fields show clearly the climatological

7 drying from spring to summer over most of North America, with the principal

8 exception over much of Mexico where the North American monsoon brings seasonal

9 rains during JJA. The models indicate that soil moisture has decreased over much of

10 North America in both seasons since pre-industrial conditions, with especially

11 robust signals during both seasons over most of Mexico and much of Canada. The

12 models suggest spring has become drier over the western Great Plains and eastern

13 Rockies of the U.S., but wetter along the West Coast. Table 3 shows that the

14 consensus decreases of soil moisture in both seasons cover a significantly large

15 portion of the continent. The same is true for the percentage of area with

16 moderately high (≥12 models) agreement on drying soils, and during JJA for very

17 high (≥14 models) consensus.

18 Similar statistics for future changes are shown in Table 4. For soil moisture,

19 corresponding to the bottom panels of Fig 2, agreement on drying is significant at all

20 thresholds of consensus, and is nearly complete during JJA. During MAM there is a

21 region of agreement near the Arctic coast for wetter soils. However over most well-

22 populated and cultivated areas, soil moisture is projected to decrease.

1   Past changes in surface heat fluxes and net radiation are shown in Fig 3. The pre-

2   industrial simulations of the models are free of anthropogenic aerosols, whereas the

3   time evolution of such emissions is provided as a boundary condition for the

4   historical experiment (Taylor et al. 2012). The signal of aerosols is very clear over

5   much of the land area from southern Canada southward. The reduced net surface

6   radiation is mainly a product of the increased shortwave optical depth in the CMIP5

7   models from the pre-industrial to the historical run. At higher latitudes, the present-

8   day warming signal is apparent as increased net surface radiation is caused by

9   greater downward longwave radiation. These changes are reflected strongly in the

10   mid-latitudes in the sensible heat flux field. In the subtropics, latent heat flux follows

11   the pattern and evolution of net radiation. At high latitudes, the changes in net

12   radiation appear to partition between both heat fluxes, favoring sensible heat

13   slightly in spring, and latent heat in summer. Field significance statistics for these

14   variables are listed in Table 3. During MAM the percentage area under various

15   portions of the negative tail of the distribution are usually significantly large. In

16   summer, the area where at least 12 models agree on increases in net radiation and

17   latent heat flux is significant, as are matching degrees of agreement for decreases in

18   both net radiation and sensible heat flux. The significant areas with changes of both

19   signs for net radiation show that the distributions do not merely shift but can also

20   spread, with extremes of different signs emerging over large but separate areas of

21   the continent.

22   Figure 4 shows the consensus for projected future changes in surface energy terms.

23   We omit the net radiation plots here – they are almost uniformly positive except

1   over the desert Southwest and North American monsoon region, where consensus is

2   weak or moderately negative (refer to Table 4 for the field significance statistics).

3   The features can be summarized as follows. The combination of strong warming and

4   greatly reduced aerosols in the RCP85 experiment lead to a strong increase in

5   available energy at the surface in most regions. Broad bands where a strong

6   consensus increase in latent heat flux corresponds to a weak-to-moderate decrease

7   in sensible heat flux align along the margin marking the accelerated snowmelt

8   margin that follows the southern edge of the retreating snowpack through the

9   season (northern U.S. and southern Canada in MAM, northern Canada and Alaska in

10 JJA). Otherwise, there is a persistent signal of increased sensible heat fluxes in both

11 seasons, agreement on reduced latent heat fluxes over Mexico and far southwestern

12 U.S. in MAM extending into the lower Mississippi Valley and Great Plains in JJA, and

13 increasing latent heat flux in boreal regions. The dominance of areas of positive

14 trends is evident in Table 4, although the southern decreases in latent heat flux are

15 able to cross the 99% confidence threshold for certain ranges of model consensus.

16 As surface fluxes are the channel by which anomalies in soil moisture are translated

17 to the atmosphere, the changes we have shown set the stage for determining trends

18 in land-atmosphere interactions from past to future. Figure 5 shows the multi-

19 model mean distribution of the terrestrial coupling index between soil moisture and

20 latent heat flux for the historical experiment (top) and the change going forward to

21 the RCP85 experiment (bottom). The climatological distribution in current climate

22 shows that regions of land-atmosphere coupling are confined to Mexico and the

23 southwestern U.S. in spring, but expand northward and eastward to encompass all

1   of the Great Plains, the Gulf Coast and some of the inter-mountain West, with a

2   maximum over Texas.

3   Changes from the pre-industrial experiment are not shown – they are mostly small

4   and noisy for JJA, but there is some coherent tendency for a decline in spring across

5   the northern U.S., in alignment with the reduced net radiation seen in Fig 3, and

6   linked to a reduction in the interannual variance of latent heat flux from pre-

7   industrial to historical cases. None of the past changes pass field significance (Table

8   3). Figure 5 shows a seesaw pattern of future change for MAM. Along the northern

9   edge of positive values of the coupling index, across the southern U.S., there are

10   positive changes that extend northward into southern Canada. The implication,

11   since this is a season of northward expansion of land-atmosphere feedbacks, is that

12   the coupling is being established earlier in the year in the RCP85 scenario. The

13   reductions at high latitudes are small in magnitude, albeit well agreed across models,

14   and do not suggest a significant change to land-atmosphere feedbacks in that area.

15   During JJA, the extensive range of robust terrestrial coupling (values greater than

16   about 9 Wm^{-2}) is largely unaffected, but all around the northern and eastern

17   margins there is consensus for future increases, suggesting the range of territory of

18   the so-called "hot spot" of land-atmosphere coupling over North America could

19   expand. Continental field significance for these changes is strong (Table 4).

20   A similar index can be constructed using sensible heat flux in place of latent heat

21   flux. The correlation between soil moisture and sensible heat flux is generally

22   negative during spring and summer, and is associated with the control of soil

23   moisture on the growth of the PBL (Betts 2004). As with the correlation between

1   soil moisture and latent heat flux, the relationship between sensible heat flux and

2   soil moisture during MMA is strong, although inverse, over Mexico and the southern

3   US, dropping to uncorrelated at high latitudes (not shown). During JJA, strong

4   negative correlations are present across North America. The changes in the RCP85

5   experiment for MAM indicate a widespread strengthening of the negative

6   correlation over most of the continent north of 30°N (not shown). This hints again at

7   a stronger role for soil moisture as a control on the overlying atmosphere, the

8   growth of the boundary layer in this case. We can quantify further the evolving

9   connection between the land surface and atmospheric boundary layer by

10   investigating the derived quantities in Eqs (2) and (3).

11   Figure 6 shows the historical multi-model mean and changes (past to present, and

12   present to future) for the height of the lifting condensation level. Z_{LCL} is largest in

13   both seasons over the Sonoran desert, but north of about 40-45°N the highest values

14   are over the longitudes corresponding with the high plains east of the Rockies. The

15   cloud base is lowest at high latitudes in spring, and over Alaska, northeastern

16   Canada and the Mid-Atlantic region of the U.S. during summer. Z_{LCL} represents the

17   depth to which the atmospheric boundary layer must grow to trigger clouds. The

18   values shown here, based on monthly mean data, are not representative of specific

19   synoptic conditions, but give a good idea of the amount of heating needed to spawn

20   convection in the absence of dynamical process in the atmosphere.

21   The CMIP5 models concur that Z_{LCL} has increased over much of the continent since

22   industrialization, except over the characteristic region of increased aerosols where

23   the cloud base has dropped. Consensus changes for JJA are generally weak, except

1   over the monsoon areas of Mexico and Central America where Z_{LCL} has increased.

2   Future projections are for higher cloud bases across North America in both seasons.

3   The overwhelming field significance for this increase is evident in Table 4.

4   Lastly, we show the changes to the Priestley-Taylor coefficient α in Fig 7. There is an

5   inverse correspondence between Z_{LCL} and α. The Priestley-Taylor coefficient is a

6   measure of the efficiency of surface evaporation into the boundary layer, and one

7   controlling factor is the gradient of humidity across the entrainment zone at the top

8   of the boundary layer. This gradient weakens as the atmospheric boundary layer

9   deepens, so that entrainment becomes less effective at reducing the moisture

10   content within the boundary layer. As a result, the humidity gradient at the bottom

11   of the well-mixed boundary layer, between the land surface and the air above it, is

12   not as effectively maintained by the mixing within the boundary layer, thus

13   hampering evaporation. However, because α also contains a factor representing the

14   evaporative fraction, controls of surface and near-surface properties (e.g.,

15   aerodynamic resistance and stomatal conductance) are also represented.

16   The mean field of α shows a gradient from low values over warm dry regions to high

17   values over cool moist regions where entrainment is most effective at maintaining

18   surface evaporation by drying the atmospheric boundary layer. Changes from pre-

19   industrial to historical experiments show areas of both positive and negative

20   changes, especially during spring. The increases over the U.S and southern Canada

21   again correspond to the region of increased aerosols. However, only the decreases

22   during summer pass field significance thresholds (Tables 3 and 4). Future changes

are uniformly negative with strong consensus among models. The match with increasing height of the lifting condensation level suggests this shift is dominated by the reduced humidity gradient across the elevated entrainment zone.

4. Synthesis

We attempt here to integrate the results found in the projected changes of land surface state variables, fluxes and derived metrics. Figure 8 shows a set of maps like those in the previous figures, defining broad areas of prevalent behavior for the two seasons and periods of simulated change by the CMIP5 models. All changes shown are based on high degrees of model consensus, and not necessarily an extraordinary magnitude of change.

The changes from pre-industrial to historical experiments are largely defined by specific regions of unitary response, such as the high-latitude warming that results in increased available surface energy, latent heat flux, and in summer drier soils and a deeper boundary layer. Spring shows many limited regions of specific responses to increasing aerosols in mid-latitudes. The west coast of the conterminous U.S. becomes rainier and soils wetter, but latent heat flux drops as this is an energy-limited regime. Across Mexico, where there is a positive feedback in the terrestrial water cycle, reduced latent heat flux accompanies drier soils and decreasing rainfall. Reduced net radiation over much of the U.S. and southern Canada has different manifestations in different areas. Across the core of the industrial belt around the Great Lakes, sensible heat is reduced and the cloud base drops. Further south

around the Ohio Valley, the boundary layer changes little despite the changes in surface heat flux.

The central Great Plains is a particularly interesting region of change. The model consensus is that precipitation has decreased since pre-industrial conditions, but latent heat flux and atmospheric boundary layer properties remain largely unchanged. In particular, α fails to increase in this area (see Fig 7). This may be an example of land use change having a direct impact, as the spread of agricultural crops into the prairies may have lowered the bulk aerodynamic and canopy resistances to moisture fluxes in this region.

The summertime changes from pre-industrial to historical conditions are more large-scale and homogeneous. There are basically three zonal bands; the high-latitude warming band with increased net radiation, the mid-latitude band of reduced net radiation and sensible heat flux where anthropogenic aerosols have increased, and the subtropical band of drying and deepening of the boundary layer.

Changes from historical to RCP85 projections seem to be defined by broad north-south dipoles in a number of fields, each with a node at a different latitude. During spring, most of North America has drier soils except along the Arctic coast. However, the line between increasing and decreasing rainfall lies much further to the south. Approximately midway between the zero lines for precipitation change and soil moisture change is a band where consensus for an increase in latent heat flux is maximum. This is also the only region of the continent where sensible heat flux is not increasing, and here the cloud base is not higher. The line dividing increasing

latent heat flux to the north from decreasing latent heat flux to the south lies near the U.S.-Mexico border. Between that line and the zero-change line for rainfall is the region where the coupling index between land and atmosphere has its maximum consensus for increase, along the northern edge of the strongest springtime coupling. However, the area over which the CMIP5 models suggest the land-atmosphere coupling will increase extends from southern Mexico to southern Canada.

During summer the nodes retreat poleward and become less zonal in orientation. Soil moisture decreases prevail over the entire continent. The line between increasing and decreasing rainfall extends from British Columbia to Hudson Bay, across Quebec and down the East Coast to the Mid-Atlantic. The line between increasing and decreasing latent heat flux remains south of the precipitation node, and the greatest consensus for increasing land-atmosphere coupling is again between them, most prevalent over the Ohio Valley and parts of the Canadian Shield. Coupling increases over most of North America north of a line a couple hundred kilometers north of the U.S.-Mexico border, and is largely unchanged south of that line.

5. Summary and Conclusions

Results of past and future projected changes to climate variables relevant to land-atmosphere interactions over North America have been presented, based on consensus among 15 CMIP5 models. Because of possible vagaries in the changes

1   simulated by specific models for specific variables, which are very difficult to

2   ameliorate in an objective fashion, all assessments are made in terms of the degree

3   of consensus among models for either a positive or negative change in each term at

4   each location. We focus on the spring and summer seasons, and assess changes in a

5   representation of past climate change (the historical experiment minus the pre-

6   industrial experiment) and extreme future climate change (RCP85 minus historical).

7   Past changes over North America as rendered by the CMIP5 models are driven by a

8   combination of three main factors – high-latitude warming from changing

9   atmospheric composition, the increase of anthropogenic aerosols over populated

10   regions with the onset of industrialization, and other regional precipitation changes

11   which appear to be occurring as the general circulation of atmosphere and ocean

12   respond to these radiative changes. The models concur that a reduction in

13   precipitation has taken place across subtropical North America since pre-industrial

14   conditions. There is also evidence for a response over the middle of the continent in

15   spring that is consistent with the effect that the expansion of agriculture over the

16   Great Plains would have on surface properties.

17   Anthropogenic aerosols appear to have delayed slightly the transition over much of

18   the continent from wintertime conditions where the atmosphere is the main

19   controller of surface fluxes to the summertime situation where soil moisture drives

20   the partitioning of net radiation between sensible and latent heat flux. This shows as

21   a general reduction in the terrestrial coupling index during MAM (see Table 3),

22   which does not pass field significance at the 99% confidence level, but would at the

23   90% level. By summer, there appears to be little change in land-atmosphere

coupling, but a reduction in sensible heat flux and cloud base over much of the mid-latitudes hints at the possibility that convective precipitation may have been inhibited somewhat with industrialization. It would be reasonable to speculate that recent indications of increasing convective rainfall and severe storms over the U.S. could be linked to cleaner air as well as increasing greenhouse gas concentrations. Sensitivity studies with climate models could examine this point further.

Future changes suggest that the springtime onset of land-atmosphere feedbacks will come earlier and penetrate further north and east into the center of the continent. This has implications for climate predictability and prediction, as anomalies in the land surface properties, such as soil moisture, can be a source of skill for forecasts on weekly to seasonal time scales. As the continent warms, sub-seasonal climate forecasts could draw more skill from land surface initialization. The growing role of land-atmosphere feedbacks could also be a contributing factor to the increased propensity toward extremes in the hydrologic cycle (e.g., more frequent and longer droughts) seen in most climate projections. This would make careful monitoring of soil moisture and other aspects of the land surface even more crucial.

The "rebound" in land-atmosphere predictability (Guo et al. 2012) that seems to set in around the first of June over the central Great Plains may begin earlier in the future. Again, it would be straightforward to test whether this would be the case using one or more climate models in properly designed experiments.

Changes in the atmospheric boundary layer during spring and summer are generally toward warmer and drier conditions (in terms of specific humidity deficit or dew-

1   point depression) and deeper development to reach a rising convective cloud base.

2   These changes reduce the impact on the boundary layer humidity of entrainment.

3   This occurs at the same time that the impact of surface fluxes and land-atmosphere

4   feedbacks enhance the impact of the land surface on the boundary layer. Thus, both

5   the absolute and relative roles of the land surface in modifying the atmosphere over

6   North America are projected to increase. In terms of local coupling between land

7   and atmosphere (Santanello et al. 2011; Dirmeyer et al. 2012b), the importance of

8   the land surface is increasing.

9   A few caveats about this analysis should be noted. The past changes simulated by

10   the models cannot be interpreted in terms of trend, because we represent them as a

11   degree of consensus among models for a certain binary change (either increase or

12   decrease) in each quantity examined. Furthermore, we use 95-year means from

13   each experiment; so we do not emphasize the later part of the historical climate

14   record where observed trends are strongest. For the future changes, we chose the

15   most extreme of the scenarios on the basis that if we find no significant impacts in

16   the most severe case, there is little chance to find effects in the more moderate

17   projections. It would be worthwhile to examine results from other representative

18   concentration pathways to see whether the responses vary linearly with the

19   strength of the radiative signal. Finally, as alluded to earlier in this section, the

20   changes found tend to implicate certain processes to a greater or lesser degree, but

21   further sensitivity studies with climate models are necessary to establish cause-

22   effect relationships with confidence.

23

13

14

1 **References:**

2 Betts, A. K., 1994: Relationship between soil moisture and vegetation in the

3   Kairouan plain region of Tunisia using low spatial resolution satellite data. *J.*

4   *Geophys. Res.*, **101**, 7209-7225.

5 Betts, A. K., 2004: Understanding hydrometeorology using global models. *Bull. Amer.*

6   *Meteor. Soc.*, **85**, 1673-1688.

7 Dirmeyer, P. A., 2006: The hydrologic feedback pathway for land-climate coupling. *J.*

8   *Hydrometeor.*, **7**, 857-867.

9 Dirmeyer, P. A., 2011a: A history of the Global Soil Wetness Project (GSWP). *J.*

10   *Hydrometeor.*, **12**, 729-749, doi: 10.1175/JHM-D-10-05010.1.

11 Dirmeyer, P. A., 2011b: The terrestrial segment of soil moisture-climate coupling.

12   *Geophys. Res. Lett.*, **38**, L16702, doi: 10.1029/2011GL048268.

13 Dirmeyer, P. A., C. A. Schlosser, and K. L. Brubaker, 2009: Precipitation, recycling and

14   land memory: An integrated analysis. *J. Hydrometeor.*, **10**, 278–288.

15 Dirmeyer, P. A., Y. Jin, B. Singh, and X. Yan, 2012a: Trends in land-atmosphere

16   interactions from CMIP5 simulations. *J. Hydrometeor.*, (submitted; draft available

17   at: ftp://cola.gmu.edu/pub/dirmeyer/AMSJHM-S-12-00141_manuscript.pdf).

18 Dirmeyer, P. A., B. A. Cash, J. L. Kinter III, T. Jung, L. Marx, C. Stan, P. Towers, N. Wedi,

19   J. M. Adams, E. L. Altshuler, B. Huang, E. K. Jin, and J. Manganello, 2012b: Evidence

20   for enhanced land-atmosphere feedback in a warming climate. *J. Hydrometeor.*,

21   **13**, 981-995.

1   Findell, K., P. Gentine, B. R. Lintner, and C. Kerr, 2011: Probability of afternoon

2   precipitation in eastern United States and Mexico enhanced by high evaporation.

3   *Nature Geoscience*, **4**, 434-439.

4   Guo, Z., and P. A. Dirmeyer, 2012: interannual variability of land-atmosphere

5   coupling strength. *J. Hydrometeor.*, (submitted).

6   Guo, Z., and co-authors, 2006: GLACE: The Global Land-Atmosphere Coupling

7   Experiment. 2. Analysis. *J. Hydrometeor.*, **7**, 611-625.

8   Guo, Z., P. A. Dirmeyer, and T. DelSole, 2011: Land Surface Impacts on Subseasonal

9   and   Seasonal   Predictability.   *Geophys.*   *Res.*   *Lett.*,   **38**,   L24812,

10   doi:10.1029/2011GL049945.

11   Guo, Z., P. A. Dirmeyer, and T. DelSole, and R. D. Koster, 2012: Rebound in

12   atmospheric predictability and the role of the land surface. *J. Climate*, **25**, 4744-

13   4749, doi: 10.1175/JCLI-D-11-00651.1.

14   Koster, R. D., and co-authors, 2004: Regions of strong coupling between soil

15   moisture and precipitation. *Science*, **305**, 1138-1140.

16   Koster, R. D., and co-authors, 2006: GLACE: The Global Land-Atmosphere Coupling

17   Experiment. 1. Overview and results. J. Hydrometeor., 7, 590-610.

18   Koster, R. D., and co-authors, 2011: The second phase of the Global Land-

19   Atmosphere Coupling Experiment: Soil moisture contributions to subseasonal

20   forecast skill. J. Hydrometeor., 12, 805–822, doi: 10.1175/2011JHM1365.1.

21   Lhomme, J.-P., 1997: An example of the Priestley-Taylor equation using a convective

22   boundary layer model. *Water Resour. Res.*, **33**, 2571-2578.

1   Santanello, J. A., C. D. Peters-Lidard, and S. V. Kumar, 2011: Diagnosing the

2   sensitivity of local land-atmosphere coupling via the soil moisture-boundary

3   layer interaction. J. Hydrometeor., 12, 766-786.

4   Taylor, K.E., R.J. Stouffer, and G.A. Meehl, 2012: An Overview of CMIP5 and the

5   experiment design. *Bull. Amer. Meteor. Soc.*, **93**, 485-498, doi: 10.1175/BAMS-D-

6   11-00094.1.

7

8

1   Table 1: Models used in this study.

Center	Model Version	Resolution
Canadian Centre for Climate Modelling and Analysis	CanESM2	128 x 64
Centre National de Recherches Météorologiques / Centre Européen de Recherche et de Formation Avancée en Calcul Scientifique	CNRM-CM5	256 x 128
Commonwealth Scientific and Industrial Research Organisation -Bureau of Meteorology	ACCESS1-0	192 x 145
Institute for Numerical Mathematics	INM-CM4	180 x 120
Institut Pierre-Simon Laplace	IPSL-CM5A-LR	96 x 96
	IPSL-CM5A-MR	144 x 143
University of Tokyo Division of Climate System Research	MIROC-ESM	128 x 64
	MIROC-ESM-CHEM	128 x 64
	MIROC5	256 x 128
Met Office Hadley Centre	HadGEM2-CC	192 x 145
	HadGEM2-ES	192 x 145
Meteorological Research Institute, Japan Meteorological Agency	MRI-CGCM3	320 x 160
NASA-Goddard Inistitue for Space Studies	GISS-E2-R	144 x 90
Norwegian Climate Centre	NorESM1-M	144 x 96
NOAA-Geophysical Fluid Dynamics Laboratory	GFDL-ESM2M	144 x 90

2
3

1   Table 2: Probabilities of various degrees of consensus among 15 models, under the
2   null hypothesis that each model returns a positive or negative change over each grid
3   box with equal probability. The local probabilities are listed in the first two rows.
4   The last row shows the thresholds for field significance over North America
5   assuming 34 spatial degrees of freedom and a confidence level of 99%.

Count	0, 15	1, 14	2, 13	3, 12	4, 11	5, 10	6, 9	7, 8
Probability	0.00003	0.00046	0.0032	0.0139	0.0417	0.0916	0.153	0.196
Cumulative Probability	0.00003	0.00049	0.0037	0.0175	0.0592	0.151	0.304	0.500
%Area of area (99% confidence)	1.76%	3.21%	5.62%	10.0%	18.3%	32.1%	50.9%	70.9%

6

7

8

Table 3. Percentage of North American land area with the indicated degree of model consensus for changes from pre-industrial to historical experiments. Situations where the area exceeds the levels expected by chance at the 99% confidence level are shown in bold.

	Models decreasing		% land	Models increasing	
	≥14	≥12	increase	≥12	≥14
MAM:					
Mean Soil Moisture	0.9%	**12.7%**	**23.4%**	1.2%	0.1%
Mean Surface Net Radiation	**7.2%**	**34.9%**	30.4%	4.5%	0.4%
Mean Sensible Heat Flux	**6.0%**	**25.1%**	36.0%	3.8%	0.2%
Mean Latent Heat Flux	0.4%	**10.6%**	39.8%	2.6%	0.3%
Coupling Index $I(w,LH)$	0.5%	8.5%	29.1%	0.7%	<0.1%
Lifting Condensation Level Z_{LCL}	<0.1%	3.2%	68.4%	**20.3%**	2.2%
Priestley-Taylor Coefficient α	1.5%	8.1%	44.2%	9.3%	1.7%
JJA:					
Mean Soil Moisture	**4.8%**	**33.9%**	**12.7%**	0.1%	0%
Mean Surface Net Radiation	**5.6%**	**21.9%**	41.9%	**10.2%**	1.3%
Mean Sensible Heat Flux	2.5%	**15.5%**	40.7%	5.3%	0.8%
Mean Latent Heat Flux	2.5%	6.1%	56.7%	**11.8%**	1.5%
Coupling Index $I(w,LH)$	<0.1%	1.2%	58.5%	3.6%	0.3%
Lifting Condensation Level Z_{LCL}	0%	0.1%	**72.6%**	9.8%	3.1%
Priestley-Taylor Coefficient α	**4.6%**	**12.1%**	33.9%	0.8%	0%

1   Table 4. As in Table 3 for changes from historical to RCP85 experiments.

	Models decreasing		% land	Models increasing	
	≥14	≥12	increase	≥12	≥14
MAM:					
Mean Soil Moisture	**33.7%**	**63.2%**	**15.6%**	0.5%	0%
Mean Surface Net Radiation	0%	1.9%	**94.3%**	**84.4%**	**44.8%**
Mean Sensible Heat Flux	<0.1%	0.2%	**80.9%**	**35.7%**	**7.1%**
Mean Latent Heat Flux	**4.2%**	10.0%	**82.7%**	**71.9%**	**28.8%**
Coupling Index $I(w,LH)$	1.8%	**16.0%**	52.5%	**23.2%**	**9.6%**
Lifting Condensation Level Z_{LCL}	0%	0%	**99.7%**	**65.5%**	**20.0%**
Priestley-Taylor Coefficient α	**45.6%**	**88.2%**	**0.9%**	0%	0%
JJA:					
Mean Soil Moisture	**41.1%**	**79.7%**	**1.2%**	0%	0%
Mean Surface Net Radiation	0%	<0.1%	**94.8%**	**70.0%**	**10.4%**
Mean Sensible Heat Flux	<0.1%	1.8%	**83.7%**	**39.9%**	**11.4%**
Mean Latent Heat Flux	1.5%	**11.3%**	61.9%	**37.0%**	**11.8%**
Coupling Index $I(w,LH)$	0%	0.4%	**83.4%**	**36.4%**	**5.6%**
Lifting Condensation Level Z_{LCL}	<0.1%	0.1%	**98.1%**	**68.7%**	**32.9%**
Priestley-Taylor Coefficient α	**62.2%**	**93.4%**	**0.1%**	0%	0%

2
3
4

1 **Figure Captions:**

2 Figure 1. JJA individual model projections of historical minus pre-industrial change

3 in soil moisture (a); 15-model mean change with equal weighting of each model (b);

4 inter-model standard deviation of JJA change in soil moisture(c); sign and degree of

5 consensus among the 15 models for the change in soil moisture (d).

6 Figure 2. Seasonal multi-model mean soil moisture from the historical experiment

7 (top); sign and degree of consensus among the models for historical minus pre-

8 industrial (middle) and RCP85 minus historical (bottom) for MAM (left) and JJA

9 (right).

10 Figure 3. Sign and degree of consensus among models for changes (historical minus

11 pre-industrial) in net radiation (top), sensible heat flux (middle) and latent heat flux

12 (bottom).

13 Figure 4. As in Fig 3 for RCP85 minus historical experiments (net radiation not

14 included).

15 Figure 5. Seasonal multi-model mean of the terrestrial coupling index from the

16 historical experiment (top); sign and degree of consensus among the models for

17 RCP85 minus historical (bottom).

18 Figure 6. As in Fig 2 for height of the lifting condensation level Z_{LCL}.

19 Figure 7. As in Fig 2 for height of the Priestley-Taylor coefficient α.

1   Figure 8. Synthesis of changes in land-atmosphere quantities for preceding (top)

2   and projected future (bottom) climate for spring (left) and summer (right). See
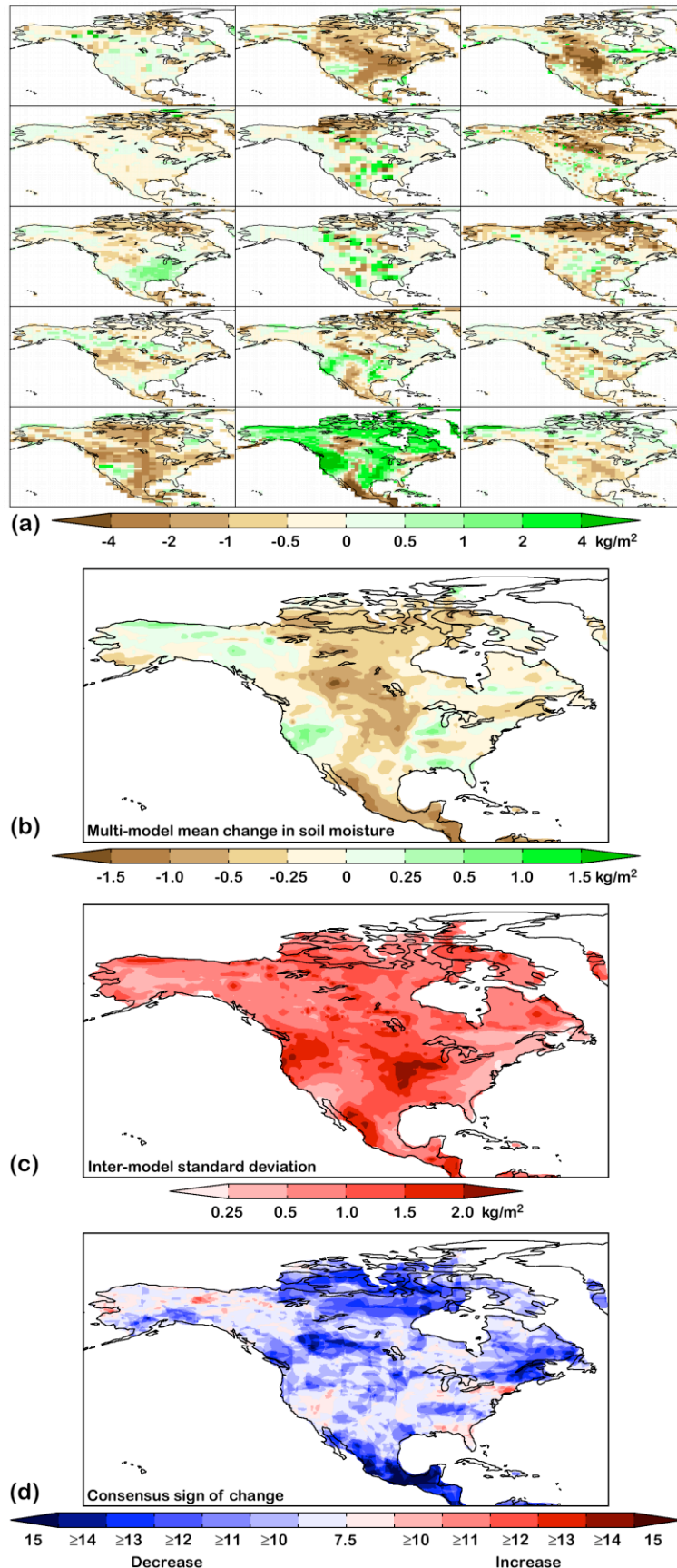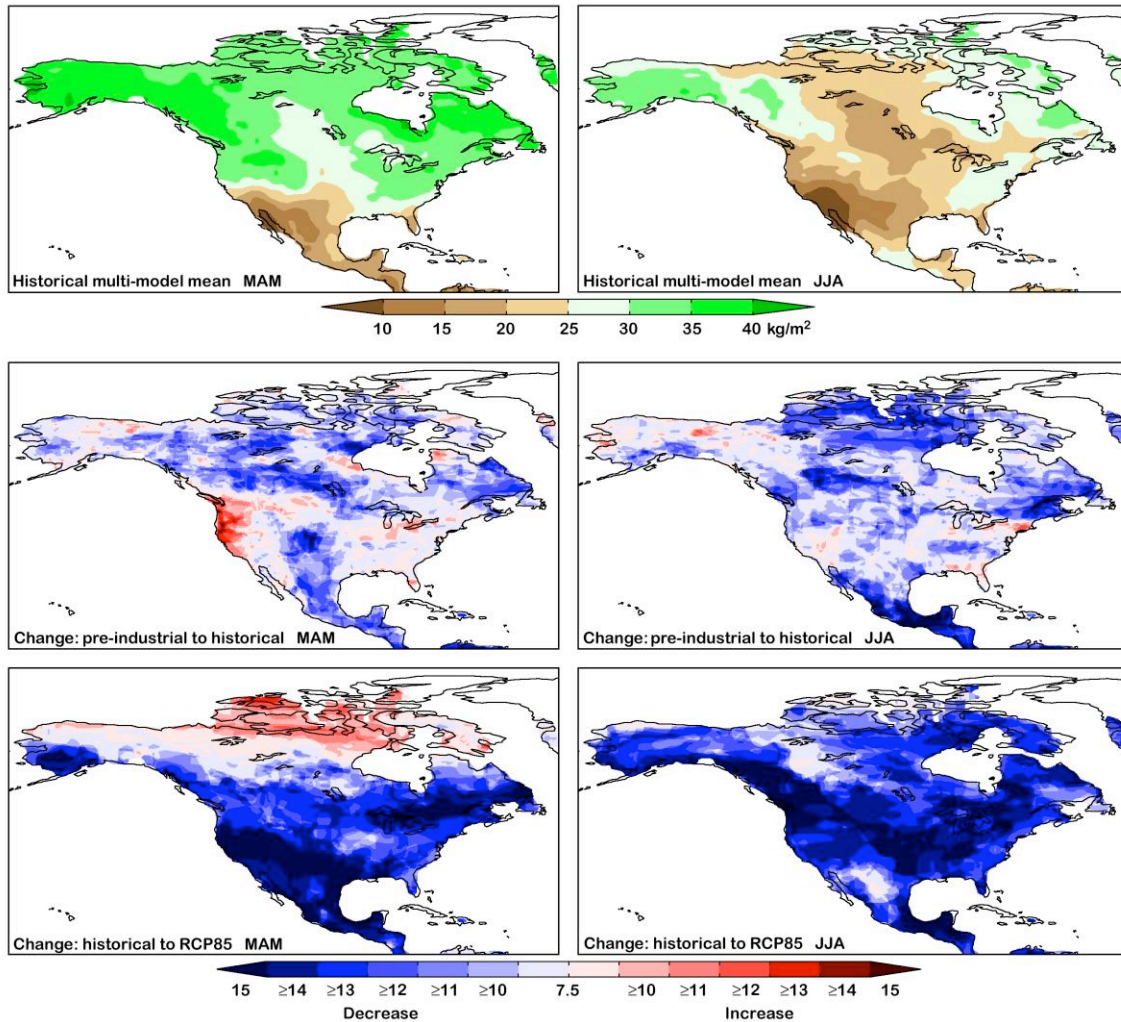
3   section 4 for details.

4

Figure 1. JJA individual model projections of historical minus pre-industrial change in soil moisture (a); 15-model mean change with equal weighting of each model (b); inter-model standard deviation of JJA change in soil moisture(c); sign and degree of consensus among the 15 models for the change in soil moisture (d).

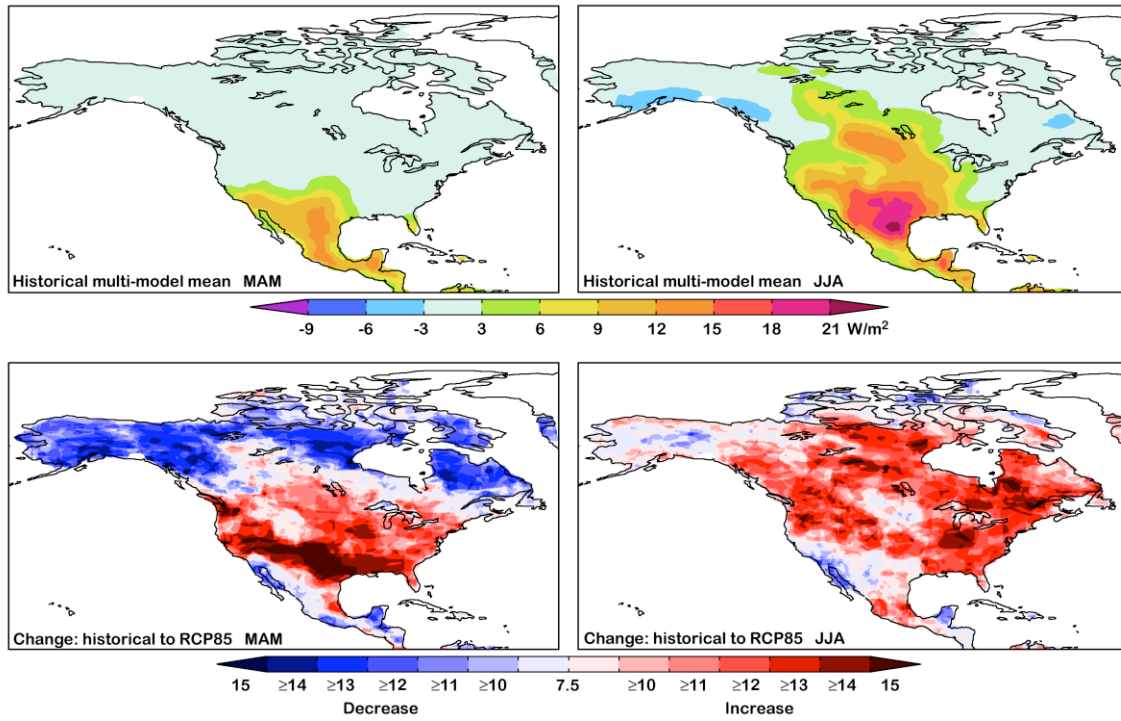Figure 2. Seasonal multi-model mean soil moisture from the historical experiment (top); sign and degree of consensus among the models for historical minus pre-industrial (middle) and RCP85 minus historical (bottom) for MAM (left) and JJA (right).
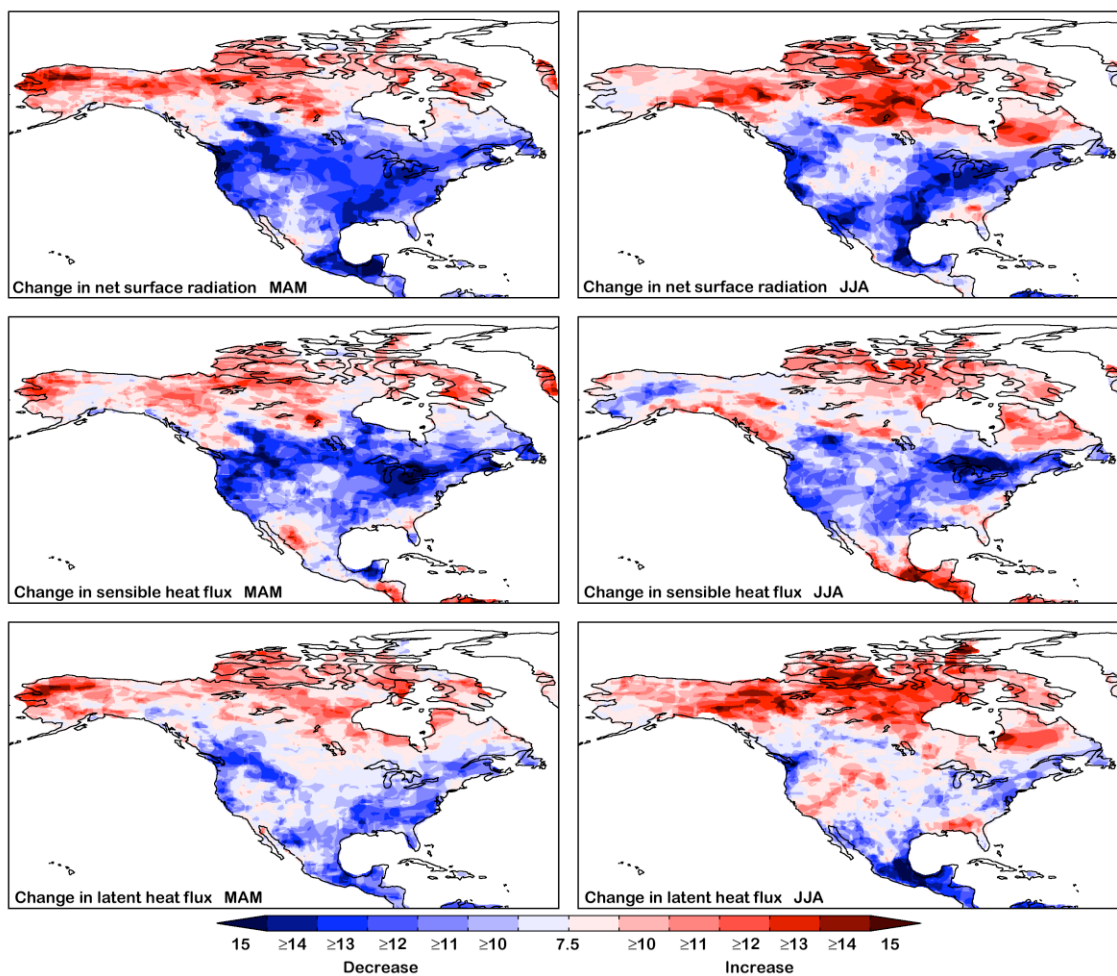
Figure 3. Sign and degree of consensus among models for changes (historical minus pre-industrial) in net radiation (top), sensible heat flux (middle) and latent heat flux (bottom).
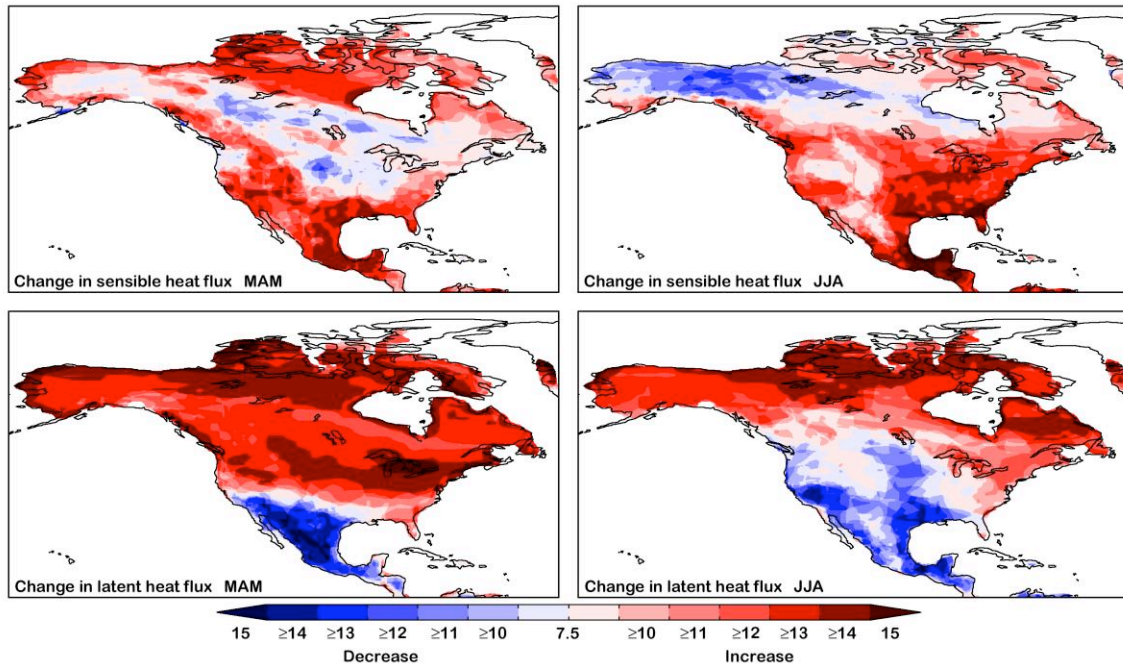
Figure 4. As in Fig 3 for RCP85 minus historical experiments (net radiation not
included).

Figure 5. Seasonal multi-model mean of the terrestrial coupling index from the historical experiment (top); sign and degree of consensus among the models for RCP85 minus historical (bottom).
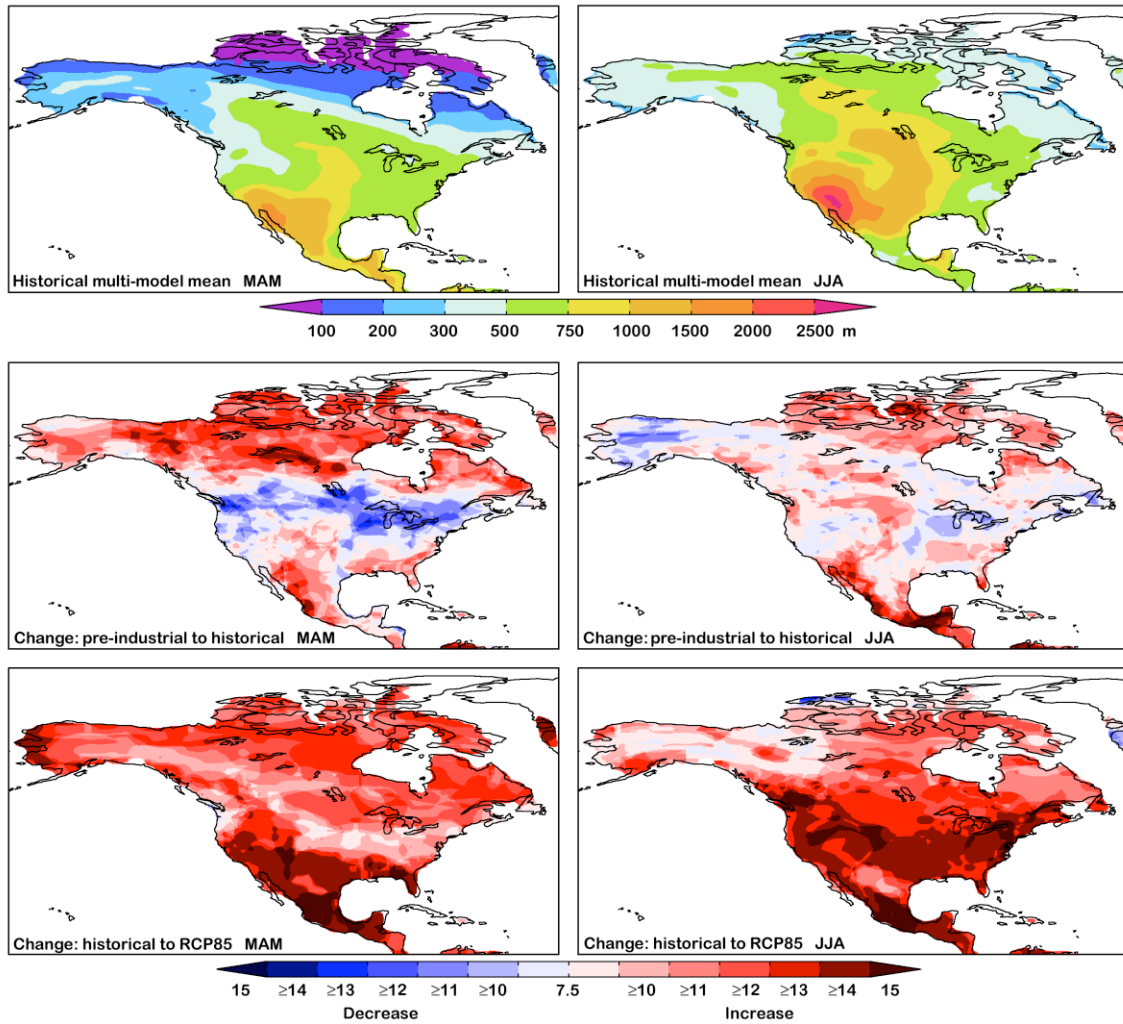
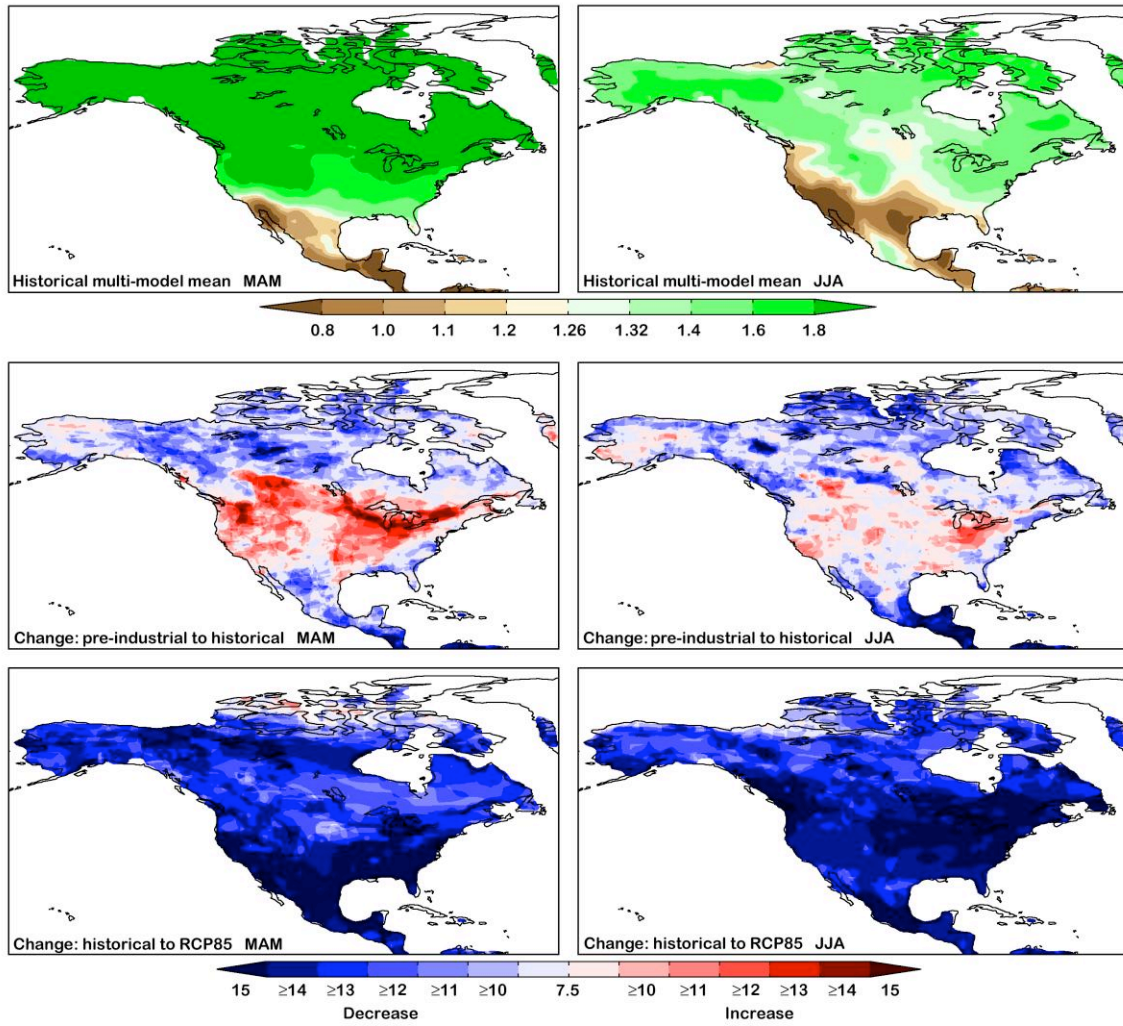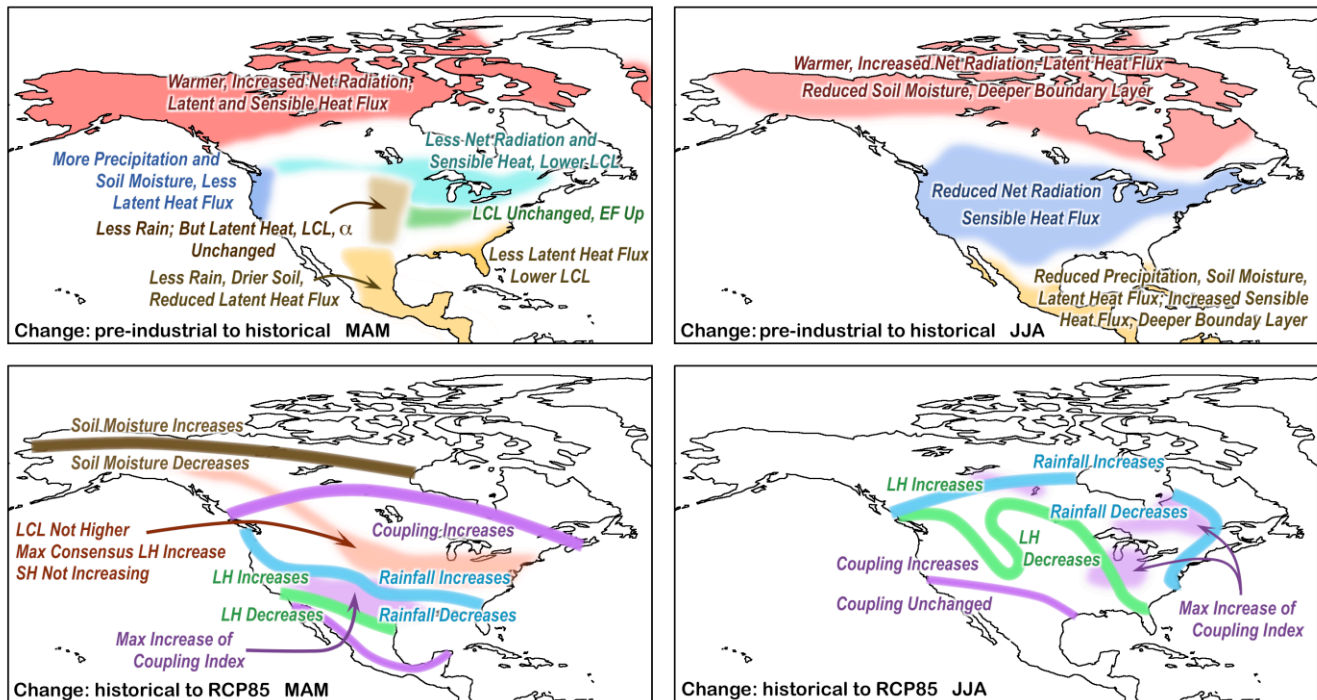Figure 6. As in Fig 2 for height of the lifting condensation level Z_{LCL}.

Figure 7. As in Fig 2 for height of the Priestley-Taylor coefficient α.

1   Figure 8. Synthesis of changes in land-atmosphere quantities for preceding (top)
2   and projected future (bottom) climate for spring (left) and summer (right). See
3   section 4 for details.
4
5